RUSH

U.S. DEPARTMENT OF COMMERCE
Patent and Trademark Office

DOCUMENT RETRIEVAL REQUEST FORM

Requester's Name: Brian Le	Case Serial Number:		Art Unit/Org.: 2623
Phone: 305 5093	Fax:	Building: PK1 4B40	Room Number:
Class/Sub-Class:			
Date of Request: 3-15-04		Date Needed By: Rush	
Paste or add text of citation or bibliography: Paste Citation		Only one request per form. Original copy only.	☐

Author/Editor:	
Journal/Book Title:	
Article Title:	SPIE
Volume Number:	Report Number: Pages: 164-80
Issue Number: V.2735	Series Number: Year of Publication:
Publisher:	
Remarks:	TK165 PS4 See attached 486765

For PTO Use Only

Monthly Accession Number:

Library Action	PTO		LC		NAL		NIH		NLM		NIST		Other	
	1st	2nd	1st	2nd	1st	2nd	1st	2nd	1st	2nd	1st	2nd	1st	2nd
Local Attempts														
Date	3/15													
Initials	CJ													
Results	NOS													
Examiner Called	IL													
Page Count														
Money Spent														

		Source	Date
Remarks/Comments 1st and 2nd denotes time taken to a library O/N – Under NLM means Overnight	Ordered From:	CIST ordered Completed Faxed	
	Comments:		

PTO-XXXX (2-96) USCOM-DC

BEST AVAILABLE COPY

Based on the result of this **study** , we propose an **HMDS** consumption reduction scheme for line-widths above 0.2 micrometer. There are many priming-related...
Identifiers: sub-0.18- mu m critical dimension **pattern** collapse...

... **HMDS** consumption reduction scheme

29/3,K/2 (Item 2 from file: 2)
DIALOG(R)File 2:INSPEC

5458601 INSPEC Abstract Number: B9702-7630-031
Title: A characterization of IHADSS performance
Author(s): **Rash, C.E. ; Harding, T.H. ; Beasley, H.H. ; Martin, J.S.**
Author Affiliation: US Army Aeromedical Res. Lab., Fort Rucker, AL, USA
Journal: Proceedings of the SPIE - The International Society for Optical Engineering Conference Title: Proc. SPIE - Int. Soc. Opt. Eng. (USA) vol.2735 p.164-80
Publisher: SPIE-Int. Soc. Opt. Eng,
Publication Date: 1996 Country of Publication: USA
CODEN: PSISDG ISSN: 0277-786X
SICI: 0277-786X(1996)2735L.164:CIP;1-1
Material Identity Number: C574-96187
U.S. Copyright Clearance Center Code: 0 8194 2116 2/96/$6.00
Conference Title: Head-Mounted Displays
Conference Sponsor: SPIE
Conference Date: 8-10 April 1996 Conference Location: Orlando, FL, USA
Language: English
Subfile: B

Title: A characterization of IHADSS performance
Author(s): **Rash, C.E. ; Harding, T.H. ; Beasley, H.H. ; Martin, J.S.**
Abstract: The performance of the **Integrated Helmet Display Sighting System (IHADSS)** used in the AH-64 Apache helicopter has been **evaluated** . Measured parameters included physical and optical eye relief, exit pupil size and position, **field -of- view** , **luminance** range, transmittance and reflectance characteristics, and static and temporal response. The purpose of the **evaluation** was to provide a performance baseline for **comparison** with future helmet mounted **display** designs.
Descriptors: aircraft **displays** ; ...

...cathode-ray tube **displays** ;
Identifiers: **integrated helmet display sighting system** ; ...

... **IHADSS** performance...

... **field -of- view** ; ...

... **luminance** range...

...helmet mounted **display** designs...

... **image** quality...
... **contrast** ratios...

... **grey** levels

A Characterization of IHADSS Performance

Clarence E. Rash

U.S. Army Aeromedical Research Laboratory
Fort Rucker, Alabama 36362-0577

Thomas H. Harding
Howard H. Beasley
John S. Martin

UES, Inc.
Fort Rucker, Alabama 36362-0557

ABSTRACT

The performance of the Integrated Helmet Display Sighting System (IHADSS) used in the AH-64 Apache helicopter has been evaluated. Measured parameters included physical and optical eye relief, exit pupil size and position, field-of-view, luminance range, transmittance and reflectance characteristics, and static and temporal response. The purpose of the evaluation was to provide a performance baseline for comparison with future helmet mounted display designs.

Keywords: test and measurement, image quality, helmet-mounted display, IHADSS

1. INTRODUCTION

The AH-64 Apache helicopter was fielded in June 1985. It is still the U.S. Army's most modern attack aircraft. Integral to the AH-64 is the helmet-mounted display (HMD) system by which the pilot and copilot view pilotage and fire control imagery. This system is known as the Integrated Helmet and Display Sighting System (IHADSS). The IHADSS consists of various electronic components and a helmet/display system, called the Integrated Helmet Unit (IHU). The IHU includes a helmet, visor housings with visors, miniature cathode ray tube (CRT), and helmet display unit (HDU) [Figure 1]. The HDU serves as an optical relay device which conveys the image formed on the CRT through a series of lenses, off a beamsplitter (often called a combiner), and into the aviator's right eye (Figure 2). The CRT is one inch in diameter and uses a P-43 phosphor. The combiner is a multilayered dichroic filter which is maximized for reflectance at the peak emission of the P-43 phosphor.

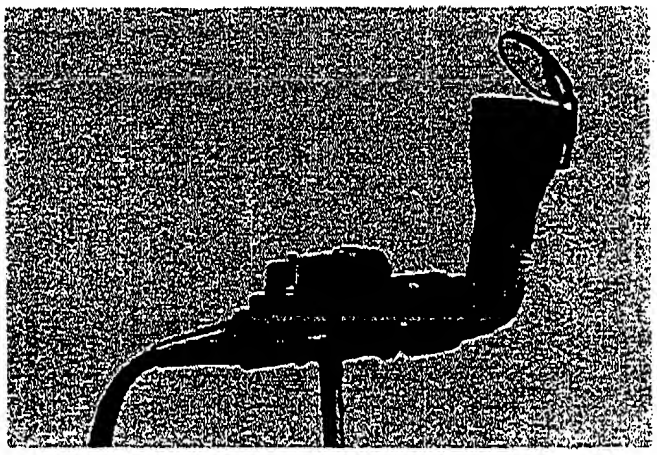

Figure 1. Helmet display unit (HDU)

0-8194-2116-2/96/$6.00

The IHADSS operates in conjunction with two forward looking infrared (FLIR) sensors located on the nose of the aircraft. One sensor, called the Pilot's Night Vision System (PNVS), provides pilotage imagery while the second sensor, the Target Acquisition and Designation System (TADS), provides targeting imagery (Figure 3). Infrared detectors, mounted on the IHU helmet, allow the FLIR sensors to be slaved to the pilot's head movements. Aircraft parameter symbology, along with the imagery from the FLIR sensor, is presented to the pilot by means of the HDU. The HDU is designed so that the image of the 30-degree vertical by 40-degree horizontal field-of-view (FOV) of the sensor subtends a 30- by 40-degree field at the pilot's eye. The IHADSS is a monocular display, presenting imagery to the right eye only. At night and under inclement weather conditions, the HDU imagery can be the sole source of information by which the pilot flies the aircraft. The visual quality of this imagery is of supreme importance.

The U.S. Army has an ongoing program for the design and fielding of a modernized reconnaissance helicopter, the RAH-66 Comanche. An improved, biocular HMD design is planned for this aircraft. To ensure an improvement in HMD performance is achieved in the new generation display, an evaluation of the HDU performance was conducted. This evaluation will be used as a baseline for comparison of future display systems. A full analysis of IHADSS performance has not been performed since the 1985 fielding of the system.[1,2]

This paper reports the results of a battery of physical image quality figures-of-merit tests performed on imagery presented on a production (April 1992) IHADSS helmet display unit and cathode ray tube. The physical evaluation of the HDU imagery consisted of the optical tests listed in Table 1. This assessment encompassed the optical characteristics of the image generation subsystem and the relay optics. The image generation subsystem consisted of a miniature, 1-inch diameter, cathode ray tube display with field flattening lens. The relay optics consisted of the prism and lenses incorporated into the barrel of the HDU and the beamsplitter (combiner lens).

Table 1.
Physical measurements of the IHADSS HDU

Exit pupil size and position	HDU spectral output
Eye relief (optical and physical)	Combiner lens transmittance/reflectance
Field-of-view	Distortion
Luminance range	Spherical/astigmatic aberration
Contrast range	Temporal response
Gray levels	Spatiotemporal MTF

2. PERFORMANCE TESTING

2.1. Exit pupil size, position and eye relief

In Figure 4, the IHADSS is shown in three configurations. In A, the HDU is shown without the combiner lens in place, while in B, the HDU combiner lens is fully retracted, and in C, the HDU combiner lens is fully extended. These three configurations constitute the three test conditions in which we made the measurements noted in the figure. Each distance measurement was made independently of any other measurement. The exit pupil diameter, P, was measured under the three conditions as was the optical distance from the objective lens to the exit pupil. In configurations B and C physical eye relief, R, also was measured. From these three configurations, certain arithmetic equalities emerge and form a basis for assessing measurement accuracy.

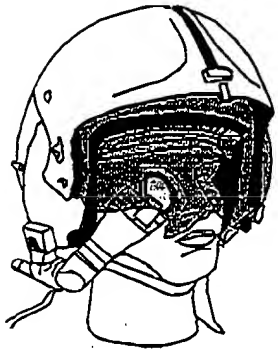

Figure 2. Aviator wearing HDU.

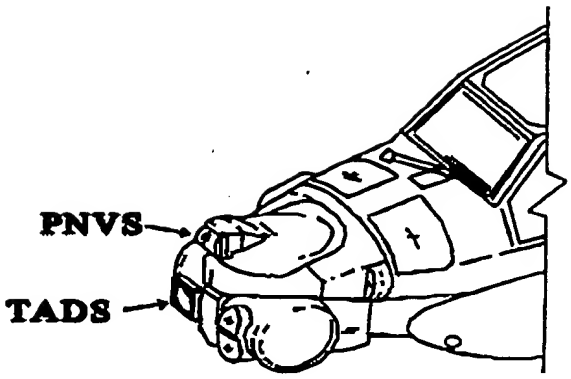

Figure 3. Nose of AH-64 helicopter with Pilot's Night Vision System (PNVS) and Target Acquisition Display System (TADS)

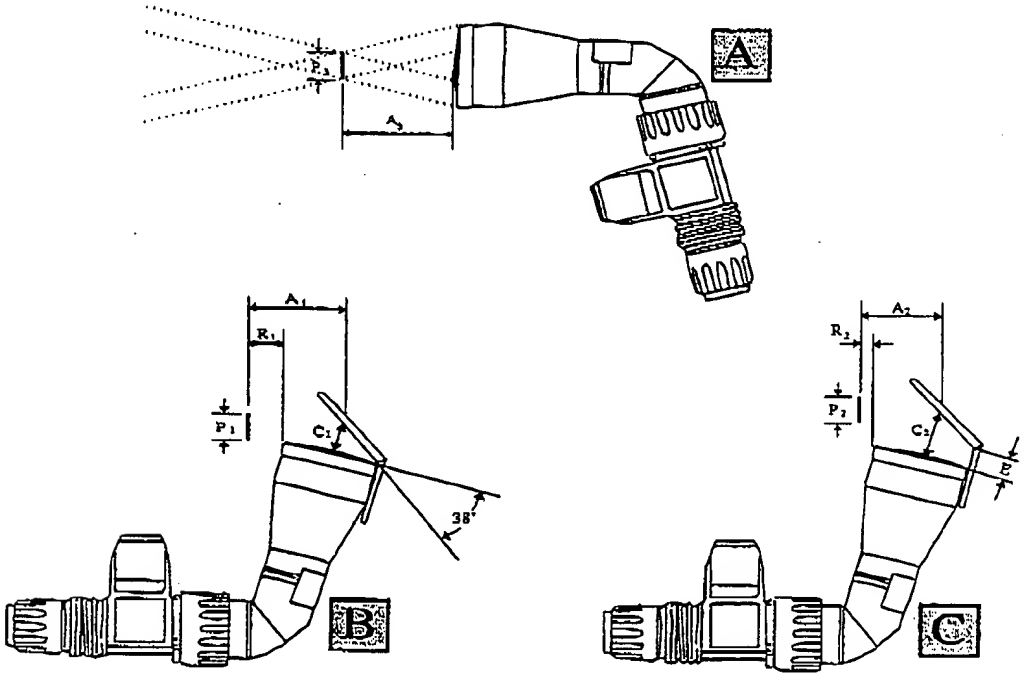

Figure 4. Schematic of physical measurement configurations of the HDU.

These identities are:

$$P_1 = P_2 = P_3 \quad (1)$$

$$A_1 + C_1 = A_2 + C_2 = A_3 \quad (2)$$

$$C_1 = C_2 - E \quad (3)$$

where A equals the distance from the exit pupil to the center of the combiner and E equals the total amount of extension available for the combiner.

For these measurements the CRT was replaced with a Honeywell, Inc. CRT simulator (P/N/ 1C1C6981-1C1), which was effectively a specially designed flashlight. The CRT simulator was designed to conform to the HDU barrel and was fitted with a field flattening lens. The CRT simulator has a test target on it that clearly shows the center of the field with crossed lines. This center target is used to optically align the HDU with a measuring telescope. The HDU has a focus adjustment which allows a minimum range of ±3 diopters. The CRT simulator did not incorporate a focus adjustment. Therefore, a diopterscope was used to confirm a minus 1 diopter setting, which was achieved using an O-ring. The selection of a minus 1 diopter setting was somewhat arbitrary, but was representative of typical pilot settings.[3]

2.1.1. Configuration A: No combiner lens

Exit pupil size. The exit pupil of the HDU was expected, by ray tracing, to be circular in shape. This would allow its size to be defined by its diameter. To measure the size of the exit pupil, we positioned the HDU, without the combiner lens in place, such that the exit pupil formed would be centered over an optical bench and optically aligned with a telescope mounted to the optical bench (Figure 5). Optical alignment was achieved by positioning the HDU until

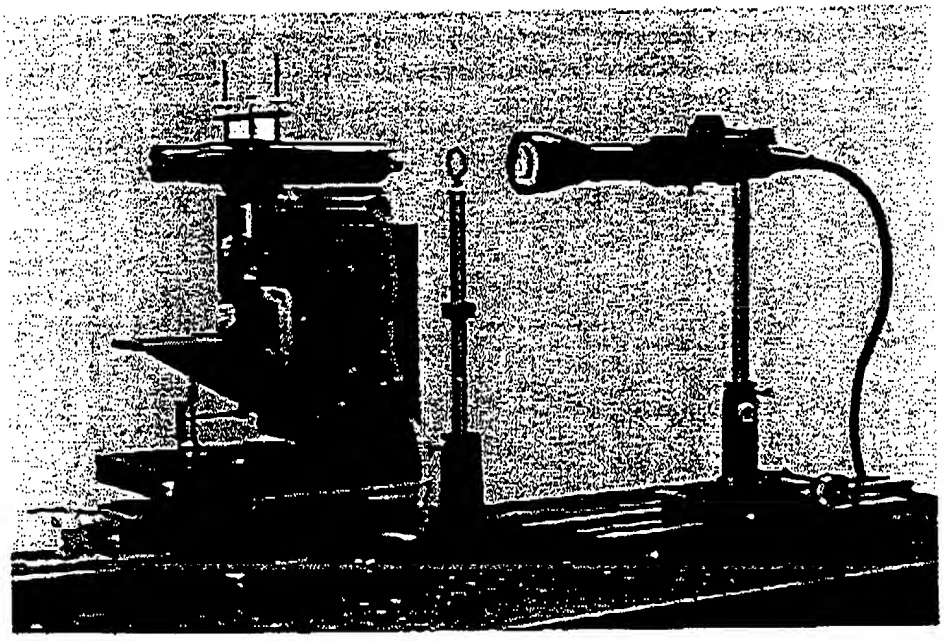

Figure 5. HDU (without the combiner lens in place) test setup for measurement of exit pupil size, position, and eye relief.

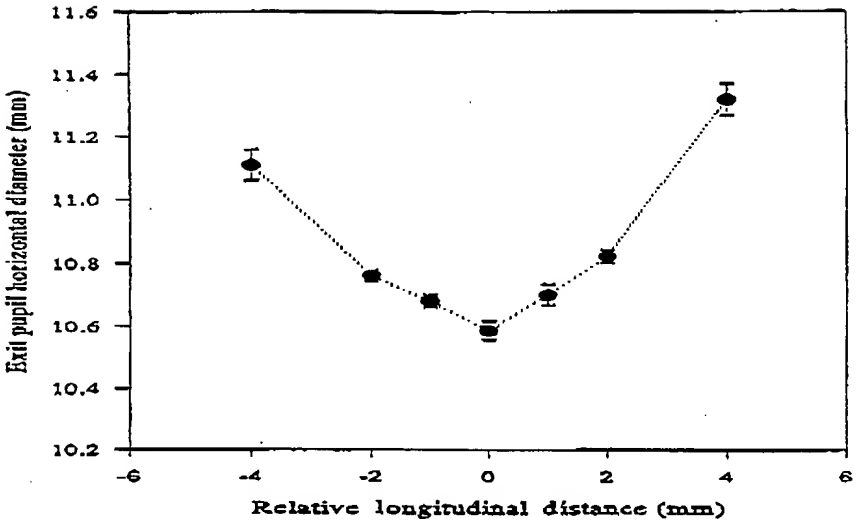

Figure 6. Behavioral assessment of exit pupil longitudinal position. Position 0 marks the position of the exit pupil. The error bars are ± 1 standard deviation.

the center of the test target was aligned with the telescope which was aligned previously to the center of the optical bench. The telescope was focused on the circular exit pupil. When viewed through the telescope, a circular disk of light was seen in sharp focus. The telescope was equipped with accurate vertical and horizontal computer driven stepping motors with 0.1-micron incremental precision. The telescope's eyepiece had a cross hair reticle with extended vertical and horizontal lines. An observer positioned the vertical cross hair on one side of the circular patch of light such that the cross hair was just tangent to the circle's outer border. The position on the stepping motor controller was set to zero and the cross hair moved to the opposite side of the patch. On this side, the cross hair was positioned just on the inside edge of the light border. In this fashion, the thickness of the cross hair would not influence our results. The distance traveled by the telescope (i.e., exit pupil diameter) then could be read from the stepping motor controller. Four additional measurements of the horizontal diameter were taken, then the procedure was repeated for the vertical diameter. The horizontal diameter measured 10.577 ± 0.023 mm and the vertical diameter measured 10.53 5 ± 0.011 mm. (Note: All error measurements are ± 1 standard deviation.) Since the measurements were so close, we combined the measures to provide our estimate of exit pupil diameter (P_3 = 10.556 ± 0.028 mm). The vertical diameter measured 10.535 ± 0.011 mm.

Exit pupil position. To measure the distance between the exit pupil and the last lens element, the objective lens, in the HDU barrel requires knowledge of the exit pupil's position in space. We developed an observer method for locating the position of the exit pupil and measuring its distance to the HDU objective lens. We aligned the HDU with the measuring telescope as above and located the approximate position of the exit pupil by moving a rear projection screen along the optical bench until we noted the exit pupil's smallest diameter imaged on the screen. Fixing the rear projection screen at this position with a linear micrometer, we focused the telescope on the image formed on the screen. The diameter of the imaged exit pupil was measured as above. The measurements were repeated until we had five independent measures of the horizontal diameter. The rear projection screen then was systematically moved fore and aft along the optical axis and the procedure repeated. During this procedure, the observer received no feedback on his performance. A graph of our results is shown in Figure 6. Note the 'V' shaped curve with the apex marking the position of the exit pupil. At the apex, the horizontal diameter of the exit pupil measured 10.586 ± 0.030 mm, which was extremely close to the 10.577 mm measured without the rear projection screen. The brackets at each data point represent one standard deviation above and below the mean of the five observations. The method yielded a highly reliable method of locating the spatial position of the exit pupil.

Placing the rear projection screen at the location corresponding to the smallest exit pupil diameter, we measured the distance from the surface of the HDU objective lens to the rear projection screen (measurement A_2). The rear projection screen was held in place by circular rings which clamped the screen between them. When viewed from the side, the thin material appeared sandwiched between the circular rings and made a highly visible and accurate target for the exit pupil position. A parallel optical bench was placed close to the one supporting the rear projection screen and telescope. A second short working distance telescope was placed on a slide positioner and the telescope aligned such that an observer could telescopically view the edge of the rear projection screen and place the vertical cross hair over it. Noting this position on the positioner, the telescope was moved, and the vertical cross hair was aligned with the side of the rear surface of the HDU's objective lens. Marking this position, we could calculate the distance traveled by the telescope and, hence, the distance from the last lens element to the exit pupil. We repeated these measurements four times, thus providing five independent measures of distance A_3. We found a mean distance of 57.660 mm with a standard deviation of ± 0.049 mm. This distance is defined as the optical eye relief.

2.1.2. Configuration B: Combiner lens retracted

Exit pupil size and position. The apparatus and test setup for the measurements depicted in configuration B are presented in Figure 7. As above, the optical telescope was mounted to the precision x-y positioning system which was in turn mounted to the optical rail, and the rear projection screen was mounted to the same optical rail via a translation rod carrier with 0.1 mm resolution. The combiner lens was mounted on the HDU and was retracted fully. The main barrel of the HDU was mounted along side the optical rail such that the combiner lens essentially was centered over the optical rail. In this position, the CRT simulator test target was aligned with the telescope cross hair. In practice, this alignment was achieved only after considerable adjustments were made to the position of the HDU. This alignment was best performed when the HDU's barrel was placed parallel to the optical axis of the telescope and screen.

The size of the exit pupil was measured using the same technique as described above by focusing on the exit pupil formed in space and measuring its horizontal and vertical diameter. Again, five independent measures of each diameter were made. The vertical diameter equaled 10.626 ± 0.022 mm and the horizontal diameter equaled 10.548 ± 0.025 mm. Averaging yielded the exit pupil diameter (P_1 = 10.587 ± 0.0451 mm).

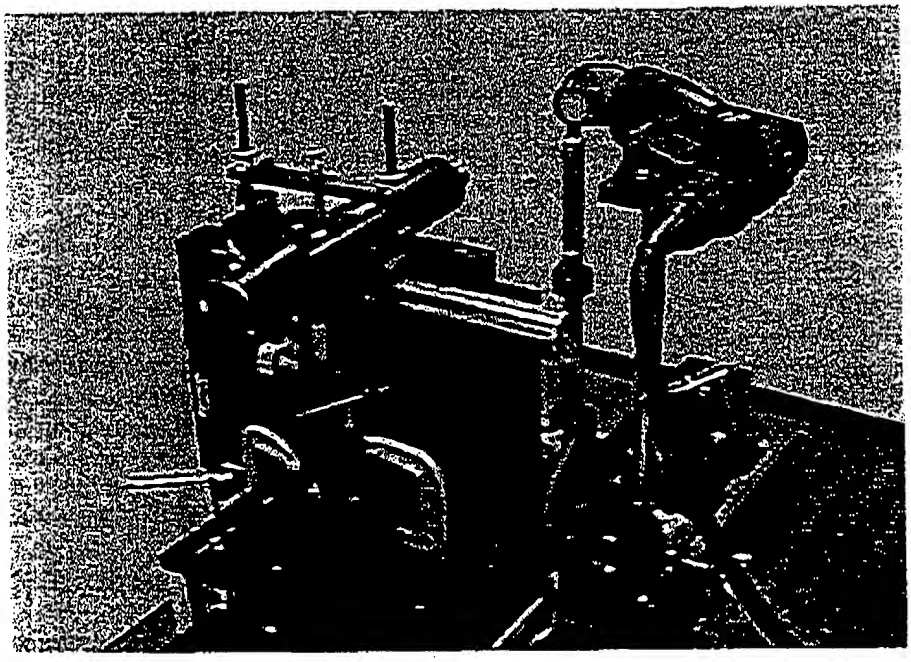

Figure 7. HDU (with the combiner lens) test setup for measurement of exit pupil size, position, and eye relief.

Eye relief. The optical eye relief of an optical system is defined as the distance along the optical axis from the last optical element to the exit pupil (measurement A_1 in Figure 4). While an important parameter to an optical designer, the optical eye relief value often is misleading. Of greater importance in helmet-mounted displays is the minimum clearance from the closest display system component to the eye or exit pupil (measurement R_1 in Figure 4). Referred to as physical eye relief or eye clearance distance, this parameter determines system compatibility with auxiliary devices, e.g., corrective lenses, protective masks, etc.

The design specification for optical eye relief for the IHADSS was that the eye relief would be at least 10 millimeters (mm) as measured from the center of the combiner lens.[4]

To measure eye relief, we first located the position of the exit pupil using the rear projection screen. Using the same technique as before, we located the position of the exit pupil to the nearest 0.5 mm. Knowing the position of the exit pupil, we measured the distance from the middle of the combiner lens to the exit pupil. The middle of the combiner lens was found by viewing the test target from a position normal to the objective lens. Focusing a telescope to infinity, we positioned the telescope such that the cross hairs and the test target center aligned properly. Focusing the telescope on the combiner lens, a marker was placed on the combiner lens at the position of the telescope's cross hair, thus marking the middle of the combiner lens. Mounting a parallel rail on the side opposite the HDU, a short working distance telescope was mounted to the parallel rail via a slide positioner and positioned to measure distances A_1 and R_1. As in our measurement of distance A_3, five independent measurements were made for each distance. We found a mean optical eye relief, A_1, of 40.12 ± 0.04 mm and a mean physical eye relief, R_1, of 13.18 ± 0.04 mm. The distance C_1, the distance from the middle of the objective lens to the middle of the combiner lens, was measured with a micrometer. This distance measured 16.12 mm.

2.1.3. Condition C: Combiner lens fully extended

Exit pupil size and position, and eye relief. Using the same test setup in Figure 7, with the exception that the combiner was fully extended, we made the measurements depicted in configuration C as presented in Figure 4. Following optical alignment of the fully extended combiner lens, the exit pupil was measured as before with a telescope mounted to a precision positioner. Following five independent measures, we found the vertical diameter equaled 10.591 ± 0.011 mm and the horizontal diameter equaled 10.502 ± 0.010 mm. Averaging yielded the exit pupil diameter (P_2 = 10.546 ± 0.046 mm). Using the rear projection screen, the position of the exit pupil was found using the pupil diameter measurement technique. The position of the telescope was moved in 0.5 mm increments. Positioning the rear projection screen at the exit pupil, the optical and physical eye relief distances (A_2 and R_2, respectively) were measured with a second telescope. Again five independent measures were made and the results were A_2 = 25.76 ± 0.049 mm, and R_2 = -5.988 ± 0.010 mm. The negative value found for R_2 means that there was a negative physical eye relief. The exit pupil was within the lateral line marked by the edge of the HDU housing at the objective lens.

The distance between the combiner lens and the objective lens, C_2, was measured with a micrometer and was found to be 32.67 mm. Also with a micrometer, the combiner extension (E) could be measured with a micrometer, and this distance was found to be 16.40 mm.

2.1.4. Consistency and accuracy of exit pupil measurements

From Equation 1, we know that P_1, P_2, and P_3 should be identical since a reflection from the combiner lens should not affect exit pupil diameter. From Table 2, we see that our measures have an average spread of 0.041 mm. This spread represents a 0.39 percent variation given a mean exit pupil diameter of 10.573 mm. From Equation 2, we find that

$$A_1 + C_1 = A_2 + C_2 = A_3. \qquad (4)$$

Substituting values from Table 2, we find a spread of 2.19 mm. This spread represents a 3.81 percent variation given a mean value of 57.44 mm. This percent variation seems high, although it should be expected when considering the difficulty of locating the exact center of the combiner lens and finding the position of the exit pupil. The position of the exit pupil was measured to the nearest 0.5 mm for P_1 and P_2 and to the nearest 1 mm for P_3.

Equation 3 relates to the combiner extension and its effect upon physical eye relief. Substituting values from Table 2 for Equation 3, we find a 0.15 mm error which represents a 0.93 percent variation from the mean of 16.195 mm. As can be seen, our measurements were free of significant error and, therefore, our measurement technique seems reliable and provides a high degree of accuracy.

Table 2.
Distance measures from Figure 4.

Measurement	Distance	Standard deviation
P_1	10.587 mm	0.045 mm
P_2	10.546 mm	0.046 mm
P_3	10.586 mm	0.030 mm
A_1	40.120 mm	0.040 mm
A_2	25.76 mm	0.049 mm
A_3	57.66 mm	0.049 mm
R1	13.18 mm	0.040 mm
R2	-5.988 mm	0.010 mm
C1	16.12 mm	N.A.
C2	32.67 mm	N.A.
E	16.40 mm	N.A.

2.2. FIELD-OF-VIEW (FOV)

Field-of-view was measured by rotating the HDU about a point that was fixed at the center of the exit pupil. By ray tracing, it can be demonstrated that the image displayed by the HDU is contained within a cone whose apex is at the exit pupil and extends out into space. By measuring luminance within this cone, we could measure the extent of the formed image. We displayed a test pattern on the HDU's miniature CRT which clearly marked the center of the CRT. By aligning a photometer with the exit pupil and with the center of this test pattern, we were able to view the test pattern as the system was rotated about the exit pupil. After this alignment was achieved, we replaced the test pattern with a uniform luminance which covered the full extent of the CRT. Adjusting the photometer to focus at the exit pupil, we could measure the luminance at the exit pupil as the HDU was rotated and thus measure the field-of-view. Figure 8 shows a plot of the luminance data. The data were relatively flat with a precipitous fall-off at the edges of the field-of-view. The horizontal field-of-view measured approximately 40 degrees and the vertical field-of-view measured approximately 31 degrees.

2.3. LUMINANCE RANGE AND CONTRAST RATIOS

The luminance range of the miniature CRTs is quite extensive although it is limited by spectral filtering, the HDU amplification circuits and the typical operational/user settings. By focusing at the exit pupil formed by the HDU, we found a maximum luminance output of 640 fL at saturation. We measured the CRT luminance loss through the

HDU to be about 46 percent which is due mainly to the elimination of the side lobes in the P-43 phosphor spectrum (Figures 9a and b). Thus the output of the CRT at saturation is about 1200 fL. We drove the CRT with an NTSC video signal where the luminance profile was a bright bar set to maximum and its leading and trailing edges set to minimum. We measured contrast ratios by focusing a photometer through the exit pupil to the center of the HDU's field-of-view (focus set to near infinity), and then the contrast was reversed and the luminance measurement repeated.

By adjusting the brightness and contrast potentiometers in the HDU amplifier to maximum, we found a contrast ratio at saturation to be about 3.0 (640/210). To define the contrast ratio over a more usable operational range, we made measurements at two peak luminance levels. The two levels we chose were 15 fL and 150 fL to correspond with lighting conditions encountered while flying with ANVIS and under daytime conditions. Operational directions on the use of the HDU indicates that brightness should be adjusted until it is just seen and then contrast adjusted to obtain differentiation between the shades of gray in a test target. With this guidance in mind, we took the following approach: with the contrast set to zero, we adjusted the peak brightness to 1 fL, measured at the target bar's peak, and then adjusted contrast until we achieved a luminance of either 15 fL or 150 fL at the peak. Under these conditions, we found contrast ratios of 13.6 (15/1.1) and 33.3 (150/4.5).

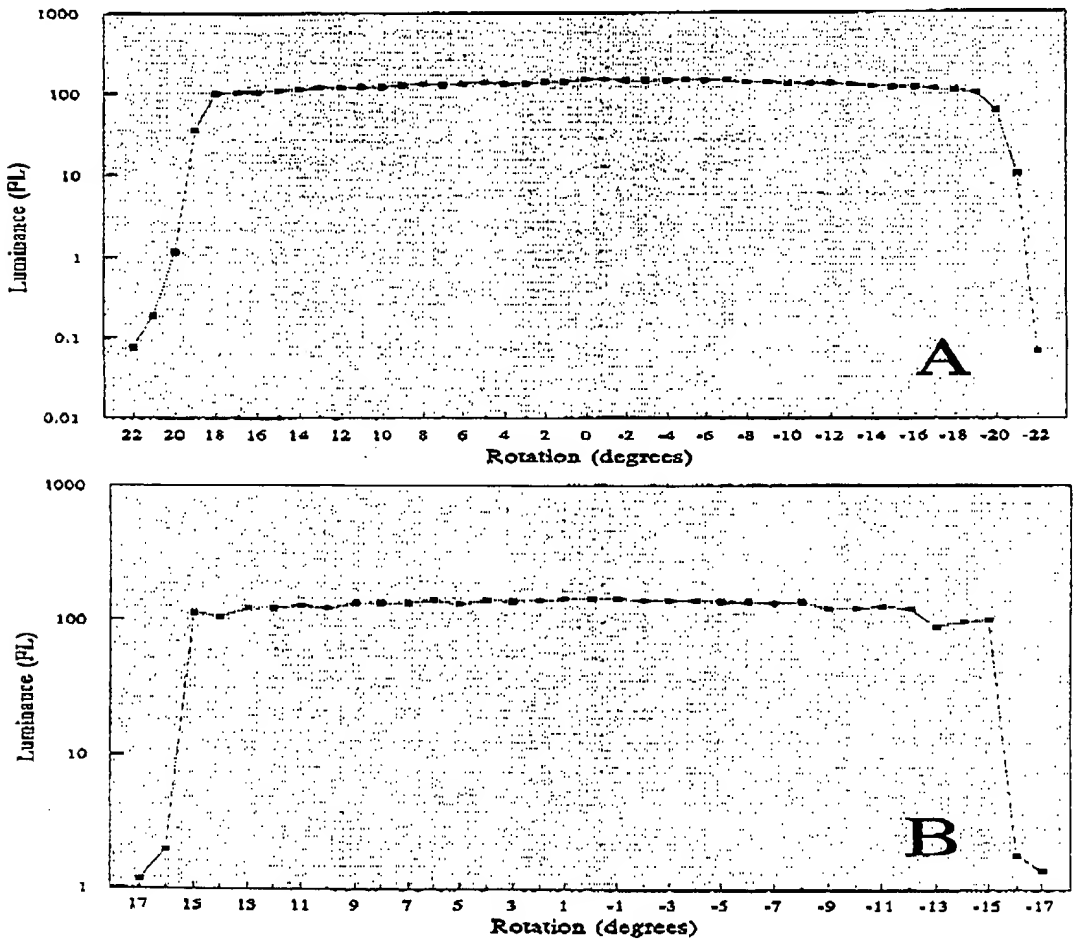

Figure 8. Luminance measurements showing the horizontal and vertical fields-of-view. A - horizontal FOV, B - Vertical FOV.

2.4. GRAY LEVELS

If we define gray levels as being discrete and one-half octave apart, then the number of gray levels can be calculated from the contrast ratios specified above. For contrast ratios of 13.6 and 33.3, we find 8 and 11 gray levels, respectively. Over the luminance range of the IHADSS, different numbers of gray levels are available. However, these two ranges offer some of the largest gray scale ranges.

2.5. SPECTRAL OUTPUT

The spectral output of the HDU was measured using a Photo Research's SpectraScan 704™ spectrophotometer and their SpectraView™ software. The spectral output of the HDU with the P-43 phosphor is narrow banded with a peak transmittance at 544 nanometers (nm) [Figure 9]. This peak corresponds with the peak of the P-43 phosphor. The width of the spectrum is about 4 to 6 nm at a level equal to 50 percent of the peak.

2.6. COMBINER SPECTRAL TRANSMITTANCE AND REFLECTANCE

The spectral transmittance of the combiner lens was measured using an EG&G Gamma Scientific RS-10A irradiance head as our light source. Its spectral output had sufficient power at each visible wavelength for reliable transmittance measurement. We used the SpectraScan 704 to measure the spectrum of the light source with and without the HDU combiner lens in the optical path. The filtered spectra was divided by the unfiltered source spectra, thus providing a transmittance curve for the combiner lens. Since the combiner lens is at an angle to the eye, we measured transmittance over a range of angular orientations. We estimate that the plane of the combiner lens is approximately 23 degrees off parallel to the front surface of the cornea. We took data from 0 to 40 degrees in 2-degree increments. Figure 10 shows the transmittance function at 22 degrees.

Assuming reflectance is equal to the light that is not transmitted through the combiner (assuming no absorption), then spectral reflectance is calculated by the following equation.

$$\text{Reflectance} = 1 - \text{Transmittance}$$

Reflectances were calculated from 0 degrees to 40 degrees. The combiner lens is coated to allow reflectance around the peak of the HDU output (544 nm with P-43 and P-53 phosphors). This peak reflectance we found to be sensitive to angular orientation. Figure 11 shows a graph of peak reflectances as a function of orientation. Note the peak shift to lower wavelengths with increasing angle. Since we measured the plane of the combiner lens to be 38 degrees off of the objective lens parallel plane (Figure 4), the data collected at that angle are most relevant. Figure 12 shows calculated reflectance at 38 degrees. The reflectance is relatively narrow band. Also plotted in Figure 12 is the spectral output of the HDU with a P-43 phosphor. The reflectance and output spectra provide a good compromise, allowing sufficient HDU luminance available to the aviator, while the broadband combiner transmittance spectra allows for adequate outside luminance to reach the aviator's eye.

2.7. DISTORTION

Distortion was measured using an Ann Arbor optical tester. The tester projected an image of a Ronchi ruling that passed through the combiner lens twice. The illuminated Ronchi ruling was positioned at the focal length of the lens which essentially collimated the light from the ruling. Moving the lens closer to the ruling increases the number of imaged lines. The light passed through the combiner, was reflected off the mirror, and passed through the combiner a second time. An image of the reflected ruling could be viewed or photographed through a lens atop the ruling. Distortion would show up as a warping or shear to the grating pattern. For the IHADSS, the ruling was clear with no apparent distortion. We examined distortion for different combiner angles, and no apparent distortion was observed.

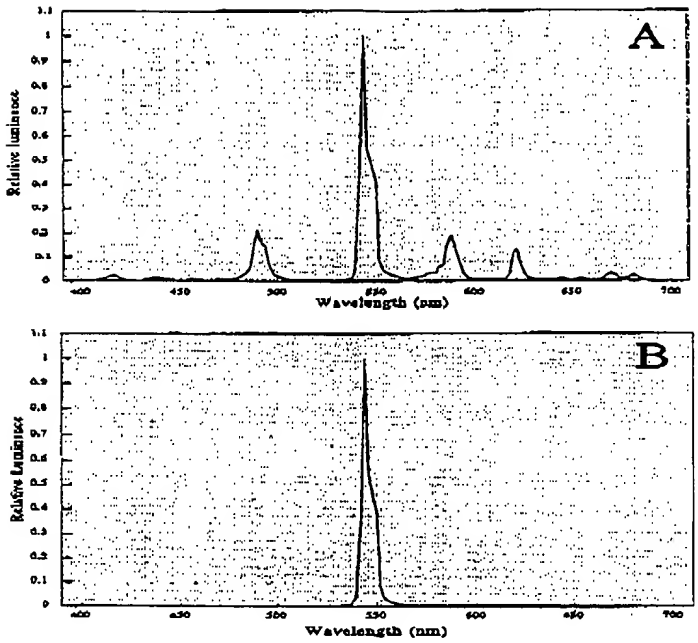

Figure 9. Spectra of a P-43 phosphor (A) and spectral output of the IHADSS HDU using a miniature P-43 phosphor (B).

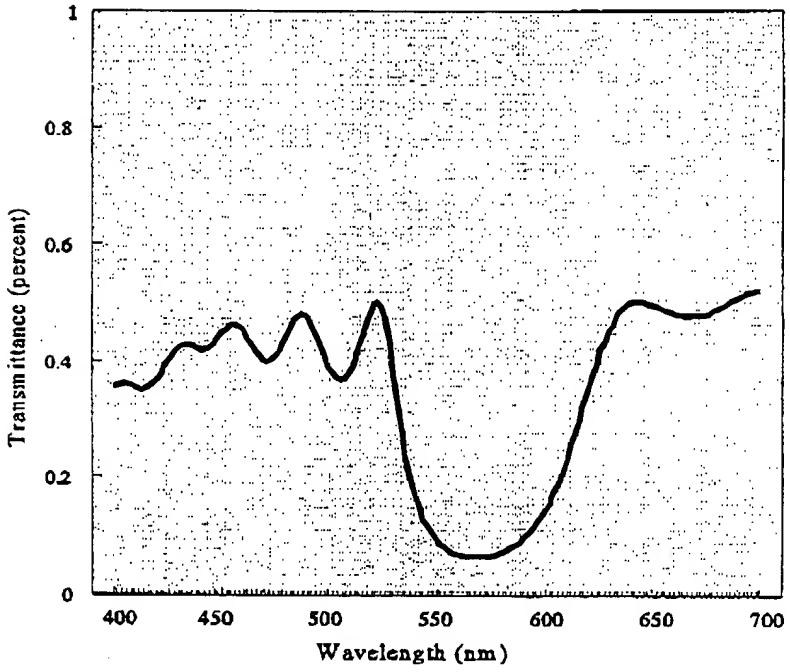

Figure 10. Combiner lens transmittance measured with the combiner lens 22 degrees off normal.

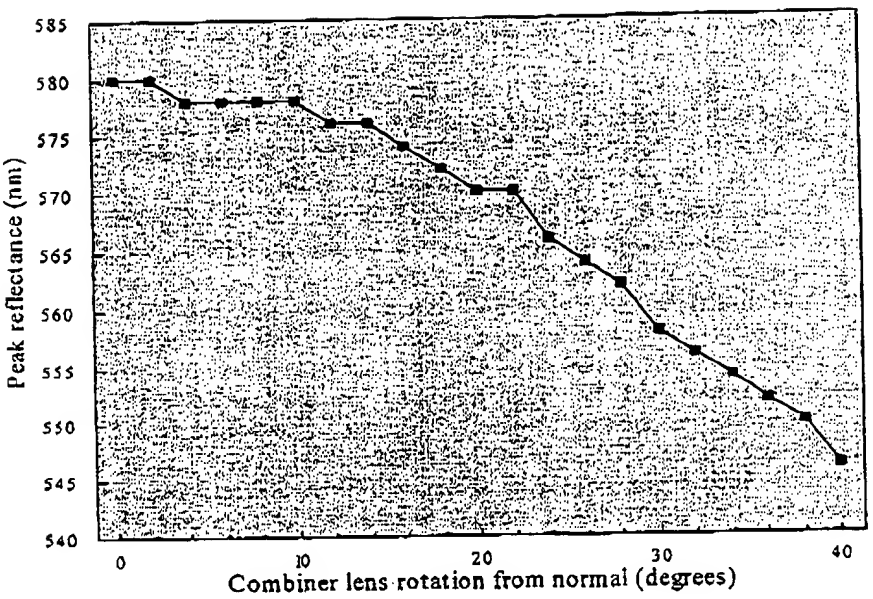

Figure 11. Combiner lens peak reflectance as a function of angular orientation.

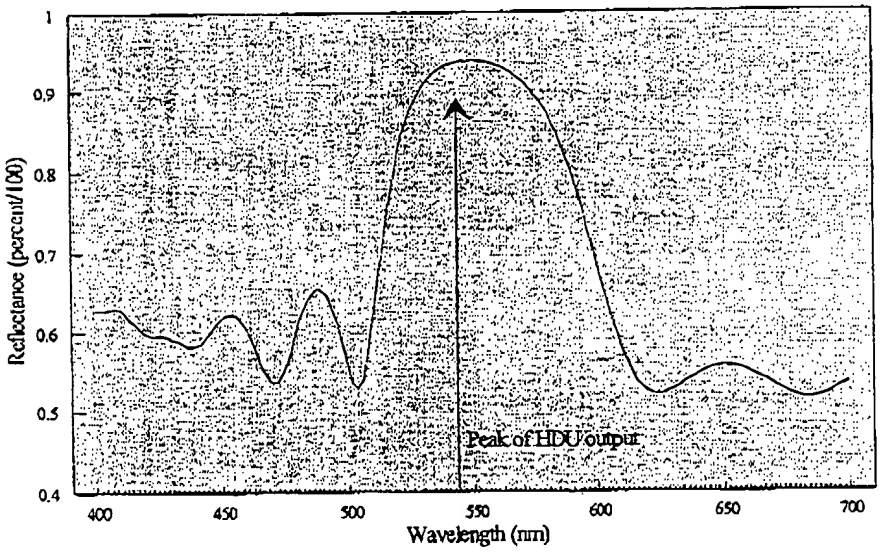

Figure 12. Combiner lens reflectance at 38 degrees off normal. Arrow marks the peak of the HDU output using a P-43 phosphor.

2.8. SPHERICAL/ASTIGMATIC ABERRATION AND FIELD CURVATURE

We measured field curvature using a dioptometer. As in the field-of-view measurements, the HDU was mounted to a rotating stage with the center of axis roughly equivalent to the position of the exit pupil. The dioptometer was mounted to the optical table and aligned with the center of the test target. The position of the exit pupil was formed at the front of the dioptometer. We adjusted the focus adjustment on the HDU until we had about a 0 diopter reading in the center of the display. During this adjustment, we took the opportunity to measure the focus range of the HDU using the dioptometer. We required auxiliary lenses to compensate for the limited two-diopter range of the dioptometer. The range of focus measured -6.25 to +3.625 diopters. Following alignment and focus adjustment, a grid of vertical and horizontal lines was displayed on the phosphor. Within each square formed by the intersecting vertical and horizontal lines, a small spot was displayed. During the course of our measurements, we noted while focusing on the lines that the spot would elongate in one direction and then the other as we went in and out of focus. This change in shape indicates an astigmatic error with the elongation of blur indicating the astigmatic axis. The axis was about 15 degrees off vertical at the 105 degree position. Therefore, we measured field curvature in the horizontal axis by focusing on the small spots. By rotating the HDU, we were able to traverse across the horizontal axis of the system. We measured field curvature by focusing on the small spots from -18 to +18 degrees, in one-degree increments (Figure 13). Field curvature is shown as a change in diopter readings as a function of degrees of rotation. Field curvature ranged from -0.5 to 1.125 diopters.

Astigmatic error was measured by rotating the grid lines to coincide with the astigmatic axis. As we traversed the horizontal axis, we focused on the 105 degree lines and then the 15 degree lines. Astigmatic aberration is the difference between the diopter readings for the two foci. We plotted the difference between the two foci in Figure 13. Note that astigmatic error exceeded 1.5 diopters in the periphery.

Spherical aberration was measured using a dioptometer mounted to a precision traversing stage. The dioptometer was aligned with the center of the test target and then the test target was replaced with a grid of vertical and horizontal lines. Dioptometer readings were made at the center by focusing on the horizontal lines and then the vertical lines. Traversing the dioptometer laterally in 1-mm increments to each side, these measurements were repeated. Spherical aberration is seen as a change in focus over the lateral positions as shown in Figure 14. As above, astigmatic aberration is the difference between the horizontal and vertical diopter readings at each lateral position from center. Data are averaged from either side of center for lateral decentration to 5 mm. At 5 mm decentration, spherical aberration was still below 0.5 diopters. On one side of center, we were able to make a measurement at 6 mm. Since the exit pupil was approximately 10.5 mm, a decentration of 6 mm would be taking a reading at the edge of the pupil. Nevertheless, we plotted these points since our readings were repeatable.

2.9. TEMPORAL RESPONSE

The temporal response of the system was measured by sinusoidally modulating a spot at multiple temporal frequencies and measuring the luminance response. The peak and trough luminance responses were used to compute Michaelson contrast, $[(L_{max} - L_{min})/(L_{max} + L_{min})]$, where L is luminance. The test spots were square test targets of increasing size (from approximately 0.2 to 1 degree square). The test targets were located in the center of the display, and their luminance was measured using a Pritchard 1980A photometer. An analog voltage signal from the photometer, whose voltage output was proportional to luminance, was fed ultimately into a Tektronix 2440 storage oscilloscope. In order to achieve a clean signal, the voltage signal from the photometer was first lowpass filtered to eliminate unwanted noise. We used two active filters with a 30-Hz cutoff frequency. The highest temporal frequency tested was 16 Hz. The peaks and troughs of the sinusoidal voltage patterns were measured, and contrast values were calculated. All of the curves had the same shape and overlapped nicely when normalized. Figure 15 shows the averaged temporal frequency curve. Unexpectedly, the curve showed no tendency for fall-off and stayed flat out to 16 Hz.

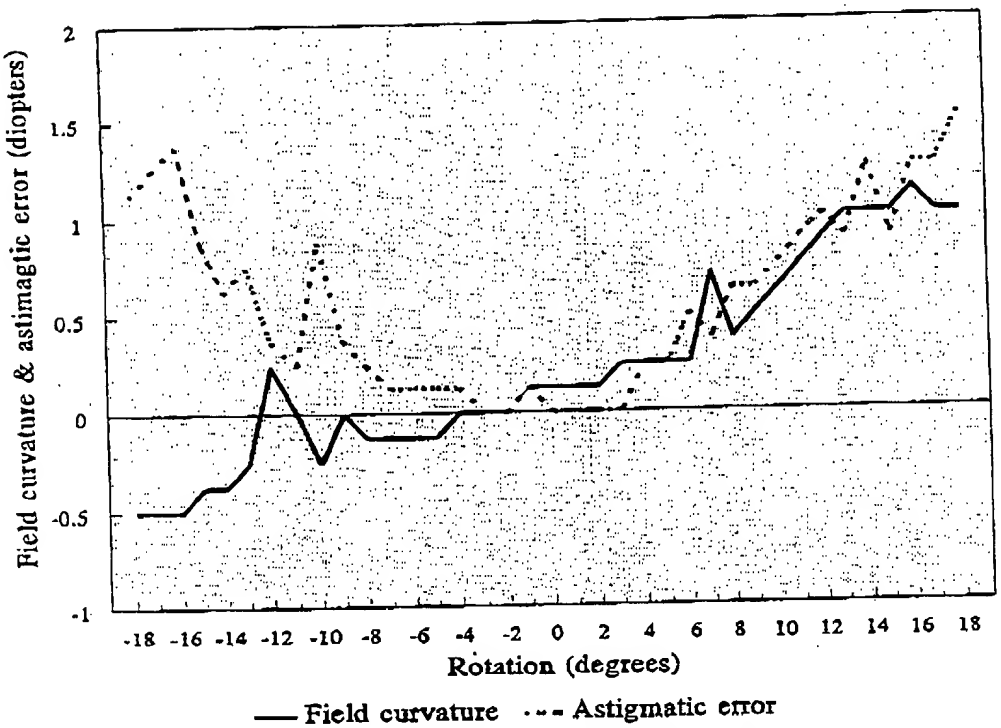

Figure 13. Field curvature and astigmatic aberration revealed as a function of degrees of angular rotation.

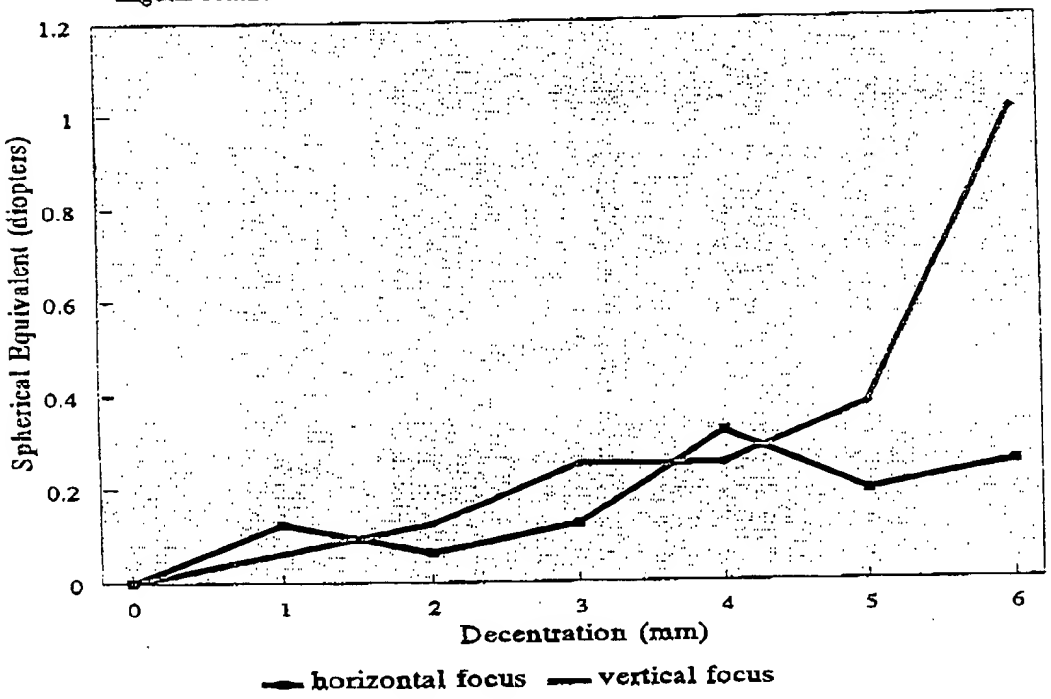

Figure 14. Spherical and astigmatic aberration as a function of decentration. Data at 6 mm may be suspect with respect to the size of the exit pupil.

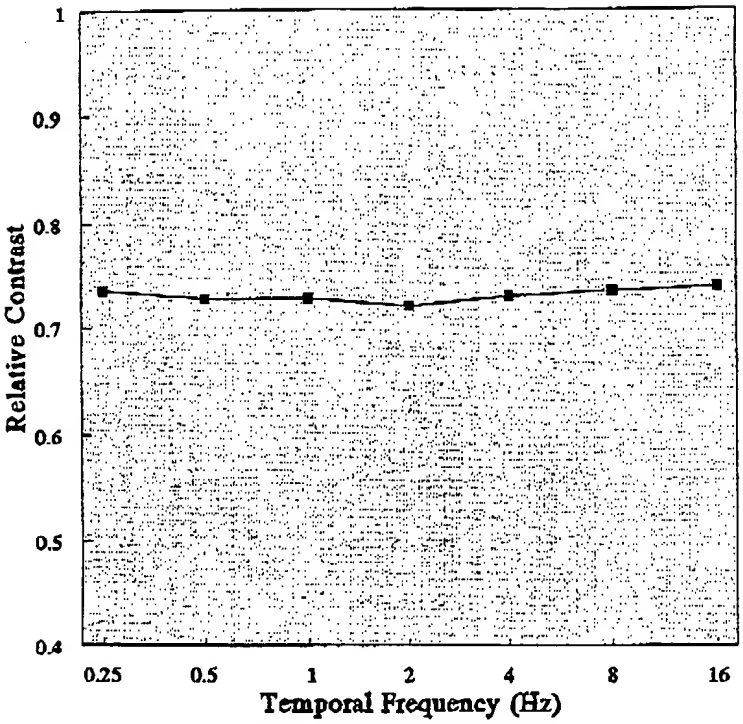

Figure 15. Temporal response of the IHADSS HDU.

2.10. SPATIOTEMPORAL MODULATION TRANSFER FUNCTIONS (MTFS)

The spatiotemporal MTF of the HDU was measured using drifting sinusoidal gratings. The gratings were generated by a Vision Research Graphics VisionWorks stimulus generator. The output from the VisionWorks system was modified to produce a standard VGA signal. Modification was made to the Texas Instruments graphics accelerator (TIGA) software drivers and to the VisionWorks software to accommodate the lower resolution VGA format. We also modified the TIGA interface board by replacing a higher frequency oscillator with a slower 28 MHz oscillator. The VisionWorks software allowed for complete control over image parameters to include spatial and temporal frequencies, size of grating patch, screen position, spatial frequency orientation, grating contrast, and either counterphase or drifting grating presentation. The video output signal was calibrated and was found to be relatively flat across all spatial frequencies.

The Pritchard 1980A photometer had a horizontal slit aperture length of only about 0.2 degrees. The photometer was focused to infinity so that the grating pattern was focused sharply. We placed a 7-mm iris in front of the photometer's objective lens which eliminated the deleterious effect of spherical aberration. Our intention was to use an iris which approximated the pupil size of human observers using the HDU, which would be on the order of 3 or 4 mm given the luminance range of the system. However, at this size pupil insufficient light would have reached the photometer, and this would have affected the temporal response of the photometer at the levels tested. We aligned the slit in the middle of the display (as marked by a test target). As with the temporal measurements, the filtered voltage output from the photometer was fed to a Tektronix 2440 storage oscilloscope and the Michaelson contrast was computed.

The nonnormalized spatiotemporal MTF of the system is shown in Figure 16. Each curve represents a different temporal frequency. As expected, there was a strong trend for decreasing contrast with increasing spatial frequency. Although the spatial frequencies seem low, our highest spatial frequency was 4.0 c/deg which corresponds to 120 cycles

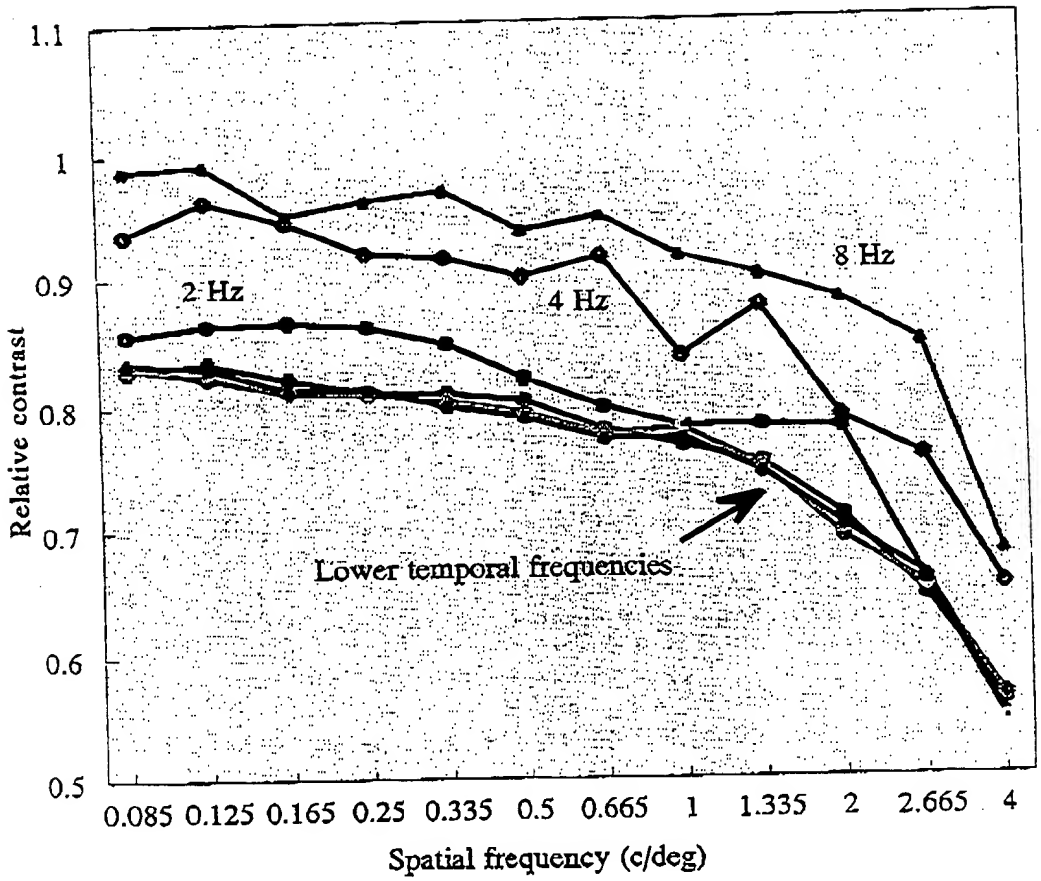

Figure 16. Spatiotemporal MTF of the IHADSS HDU.

per vertical display height. We found that low temporal frequency curves overlapped well, but the curves at 4 Hz and 8 Hz showed a significant increase in contrast (approximately 10 percent and 15 percent increase, respectively). This rise in contrast at the high temporal frequencies was not expected since we saw no significant rise in the temporal response curves (Figure 15). We have no reasonable explanation for this high temporal frequency effect.

3. DISCUSSION

The IHADSS has been successfully fielded for a decade now, and its performance forms a basis for comparing all future HMD systems. To better understand the performance characteristics of the IHADSS HDU, we undertook this project to quantify important physical characteristics and performance figures-of-merit. We examined the optical characteristics of the HDU to include physical and optical eye relief, exit pupil characteristics, light transmittance and reflectance, optical aberrations, and field-of-view. We also examined the performance characteristics of the IHADSS imagery to include luminance range and available gray shades, spectral output of IHADSS imagery, and spatial and temporal response characteristics.

The exit pupil formed by the HDU was found to be about 10.5 mm in diameter and positioned approximately 57 mm behind the HDU's objective lens. The 57-mm optical path length provided an optical eye relief of about 40 mm with the combiner lens retracted and about 26 mm with the combiner fully extended. Of more importance, physical eye relief also was measured for the two combiner lens positions. With the combiner lens retracted, physical eye relief measured about 13 mm. With the combiner lens fully extended, however, we found a negative physical eye relief of about 6 mm.

The field-of-view of the HDU measured approximately 40 degrees by 31 degrees by interpreting the luminance curves shown in Figure 8. The luminance output of the HDU was quite high (luminance saturation equaled about 600 fL). Setting the maximum to 15 and 150 fL, we found contrast ratios of 13.6 and 33.3 which provided a respectable 8 and 11 gray shades, respectively.

The spectral output of the HDU was narrow banded and peaked at 544 nm, corresponding to the peak of the P-43 phosphor. The combiner lens forms an approximate 38 degree angle to the barrel of the HDU. At 38 degrees, the spectral reflectance is banded and peaks at 550 nm. At this angle, about 90 percent of the light emitted from the HDU is reflected into the eye. The combiner forms an angle which is about 23 degrees off normal to the visual line of sight. At this angle, the transmittance is relatively low, and at 544 nm, about 10 percent of the light is transmitted to the eye.

Optically, the IHADSS is a relatively good system. Spherical aberration was certainly low and of little consequence. However, our measurement of field curvature showed a full diopter increase in the periphery with quite noticeable astigmatic aberration. The astigmatic axis was located at about 105 degrees.

The temporal response of the HDU was superb. The temporal response function was flat out to 16 Hz which was the highest frequency tested. The spatiotemporal MTF likewise showed a superb temporal response. Spatially, we saw the anticipated reduction in contrast with increases in spatial frequency. At 4 cycles/deg, contrast was down to about 70 percent of maximum. Since the symbology displayed on the HDU generally is comprised of low spatial frequencies, this fall-off of contrast does not seem to be of significant consequence.

4. ACKNOWLEDGMENTS

This work was partially supported by the U.S. Army Medical Research and Materiel Command under Contract No. DAMD17-95-C-5095.

5. DISCLAIMER

The views, opinions and/or findings contained in this report are those of the authors and should not be construed as an official Department of the Army position, policy, or decision unless designated by other documentation.

6. REFERENCES

1. C.E. Rash, J.L. Haley, T.A. Hundley, W.E. McLean, and B.T. Mozo, "Prototype testing of the Integrated Helmet Unit for the Integrated Helmet and Display Sighting System," U.S. Army Aeromedical Research Laboratory, USAARL LR 82-6-2-1, 1982.

2. C.E. Rash, J.L. Haley, W.E. McLean, and B.T. Mozo, "Production item testing of the Integrated Helmet Unit for the Integrated Helmet and Display Sighting System," U.S. Army Aeromedical Research Laboratory, USAARL LR 84-7-2-3, 1984.

3. I. Behar and C.E. Rash, "Diopter focus adjustment of Apache IHADSS," Aviation Digest, p. 14-15, Vol. 1-90-1, 1990.

4. Hughes Helicopters, Inc., Procurement specification for the production Integrated Helmet and Display Sighting System (IHADSS), PS-14-11077D, 16 March 1982.